

A drop in the ${}^6\text{Li}(p, \gamma){}^7\text{Be}$ reaction at low energies



J.J. He^{a,*}, S.Z. Chen^{a,b}, C.E. Rolfs^{c,a}, S.W. Xu^a, J. Hu^a, X.W. Ma^a, M. Wiescher^d,
R.J. deBoer^d, T. Kajino^{e,f}, M. Kusakabe^g, L.Y. Zhang^{a,b}, S.Q. Hou^{a,b}, X.Q. Yu^a, N.T. Zhang^a,
G. Lian^h, Y.H. Zhang^a, X.H. Zhou^a, H.S. Xu^a, G.Q. Xiao^a, W.L. Zhan^a

^a Institute of Modern Physics, Chinese Academy of Sciences, Lanzhou 730000, China

^b University of Chinese Academy of Sciences, Beijing 100049, China

^c Fakultät für Physik und Astronomie, Ruhr-Universität Bochum, Bochum 44780, Germany

^d Department of Physics, University of Notre Dame, Notre Dame, IN 46556, USA

^e National Astronomical Observatory of Japan, Mitaka, Tokyo 181-8588, Japan

^f Department of Astronomy, Graduate School of Science, University of Tokyo, Hongo, Bunkyo-ku, Tokyo 113-0033, Japan

^g Institute for Cosmic Ray Research, University of Tokyo, Kashiwa, Chiba 277-8582, Japan

^h China Institute of Atomic Energy, P.O. Box 275(1), Beijing 102413, China

ARTICLE INFO

Article history:

Received 30 October 2012

Received in revised form 18 July 2013

Accepted 18 July 2013

Available online 25 July 2013

Editor: V. Metag

Keywords:

Radiative capture

Direct capture

S factors

Big-bang nucleosynthesis

ABSTRACT

The low-energy astrophysical S factors of the ${}^6\text{Li}(p, \gamma){}^7\text{Be}$ reaction have been investigated on a 320 kV platform at the Institute of Modern Physics in Lanzhou. The experimental S factor of this reaction shows an interesting sizable drop contrary to any existing theoretical expectations at energies below 200 keV. Such drop has not been fully understood yet and may reflect a novel reaction mechanism. The appearance of an interesting new positive-parity $1/2^+$ or $3/2^+$ resonance at $E_{\text{c.m.}} \approx 195$ keV is discussed. This study shows the danger of extrapolating experimental data over too large an energy range and demonstrates the need for careful direct experimental studies of reaction cross sections at or near stellar energies. In addition, our new results are discussed in the framework of a SUSY assisted Big-Bang Nucleosynthesis (BBN) model.

© 2013 Elsevier B.V. All rights reserved.

Nuclear astrophysics strives for a comprehensive picture of the nuclear reactions responsible for synthesizing chemical elements and for powering the stellar evolution engine. Thereinto, the measurements of nuclear reaction cross sections (expressed as S factors) at stellar Gamow energies are of great importance to nuclear astrophysics [1]. A lot of investigations have been done in the past fifty years (e.g., see compilation [2]), even in an ultra-low background deep underground facility LUNA [3]. It reveals that the experimental S factors at low energies sometimes show quite different behaviors comparing to simple extrapolation from the extensively studied high-energy data. For instance, for the ${}^2\text{H}(d, \gamma){}^4\text{He}$ reaction involved in both primordial and stellar nucleosynthesis [4,5], its astrophysical S factor was thought to decrease steeply with decreasing energy based on the theoretical predictions. However, the experimental results [6,7] show a significantly higher S factor (about 32 times) than theoretical expectation because of the ${}^4\text{He}$ D -admixture. It demonstrates clearly the danger of extrapolating experimental data over a very large energy range towards stellar energies.

olating experimental data over a very large energy range towards stellar energies.

The ${}^6\text{Li}(p, \gamma){}^7\text{Be}$ reaction has been studied previously over a wide energy range down to about center-of-mass (c.m.) energy of $E_{\text{c.m.}} = 140$ keV ([8] and references therein). The non-resonant data were well described by the direct capture model except one lowest data point at 140 keV [2]. In addition, an analyzing-power measurement [9] for this reaction indicated that the S factor had a negative slope towards low energies, while a thick-target measurement with a γ -to- α branching ratio method indicated a positive slope [10]. However, the extrapolated S factors for both measurements deviated dramatically from those experimental ones [8] around $E_{\text{c.m.}} = 200$ keV. Furthermore, there is a well-known problem for many years that a positive parity resonance seems to be necessary to explain the unusual angular distributions measured for ${}^6\text{Li}(p, \alpha){}^3\text{He}$, but such a resonance has not been discovered yet [11–15]. With regard to the nuclear astrophysical aspect, current models of stellar evolution predicted negligible quantities of ${}^6\text{Li}$ in the hydrogen burning phases of stellar evolution [16]. Primordial, or standard and inhomogeneous big-bang nucleosynthesis (BBN) [17,18] might have been more generous in its production of

* Corresponding author.

E-mail address: jianjunhe@impcas.ac.cn (J.J. He).

this element within an effective temperature region of 1–0.1 GK. For example, a low quantity of ${}^6\text{Li}$ can survive in the BBN according to Schramm and Wagoner's estimation [19]. In addition, in a recently developed SUSY assisted BBN model [20] and references therein, the non-thermal photon-induced reaction ${}^7\text{Be}(\gamma_{\text{nt}}, p){}^6\text{Li}$, whose cross section is larger than that of ${}^7\text{Be}(\gamma_{\text{nt}}, \alpha){}^3\text{He}$ for γ_{nt} energies higher than ~ 10 MeV, can efficiently destroy ${}^7\text{Be}$ and produce ${}^6\text{Li}$, where γ_{nt} is the non-thermal photons which are produced from SUSY particle decay. The cross section of ${}^7\text{Be}(\gamma, p){}^6\text{Li}$ is, however, not expected to affect the ${}^7\text{Be}$ abundance. This is because the threshold energy of ${}^7\text{Be}(\gamma, p){}^6\text{Li}$ ($Q = 1.587$ MeV) is smaller than that of ${}^7\text{Be}(\gamma, \alpha){}^3\text{He}$ ($Q = 5.606$ MeV) so that a soft non-thermal photon spectrum generated by the radiative particle decay prefers ${}^7\text{Be}$ destruction via the former reaction. On the other hand, the cross section possibly affect significantly the ${}^6\text{Li}$ abundance, which can characteristically be elevated in this model with respect to the standard BBN model [20]. Since the low-energy cross section of the ${}^6\text{Li}(p, \gamma){}^7\text{Be}$ reaction is related to that of the ${}^7\text{Be}(\gamma, p){}^6\text{Li}$ inverse reaction through the principle of detailed balance, the theoretical calculations of the BBN model would benefit from an improved determination of the cross section of ${}^6\text{Li}(p, \gamma){}^7\text{Be}$. Therefore, the measurement of capture cross section of ${}^6\text{Li}(p, \gamma){}^7\text{Be}$ will permit the production of ${}^7\text{Be}$ and ${}^6\text{Li}$ in these scenarios to be well evaluated [10,21].

With these considerations in mind, it is worthwhile to measure the low-energy cross sections of ${}^6\text{Li}(p, \gamma){}^7\text{Be}$ reaction ($Q = 5.606$ MeV [22]) to clarify the above discrepancy and controversy as well as to reveal the astrophysical implications. This Letter reports our new direct S -factor measurement results for this reaction in the center-of-mass energy range from 51 to 257 keV, corresponding to a Gamow temperature region of 0.1–1.1 GK. We have discussed the novel reaction mechanism, the structure implied as well as the astrophysical implications in relation to our new results.

The experiment was carried out at the 320 kV platform [23,24] for multi-discipline research with highly charged ions at the Institute of Modern Physics in Lanzhou. New experimental results cover the reaction cross section in the proton energy range of 70–300 keV. For technical reasons, *i.e.*, high voltage stability, we measured the cross sections below about 300 keV, where the stability was better than 0.1 kV. The experimental setup is similar to the one described in Ref. [25], and will be described in details elsewhere [26]. The proton beam (current up to 30 μA) passed through 2 collimators (each 10 mm in diameter) and was focused on the target. The two collimators were located 50 and 100 cm upstream of the target. The solid targets were prepared from ${}^6\text{Li}_2\text{O}$ material evaporated onto a 0.5 mm thick Ta backing, with a ${}^6\text{Li}$ enrichment of 95% and a thickness of 35 $\mu\text{g}/\text{cm}^2$, measured via a quartz crystal monitor. The targets were directly water cooled. An inline Cu shroud cooled to LN_2 temperature (a pipe of 4 cm in diameter) extended close to the target for minimizing carbon build-up on the target surface. Together with the target, it constituted the Faraday cup for beam integration. The typical vacuum pressure of the target chamber was about 4×10^{-7} mbar. A negative voltage of 250 V was applied to the pipe to suppress secondary electrons from the target. The energy of the proton beam was calibrated using a well-known 149 keV resonance in ${}^{11}\text{B}(p, \gamma){}^{12}\text{C}$, and the accuracy was better than ± 0.2 keV [26].

The capture γ rays were observed using a segmented Clover detector [27] with relative efficiency of about 200% at $E_\gamma = 1.3$ MeV, placed in close geometry at zero degrees with its front face at a distance of 4 cm from the target. The energy calibration of the detector was obtained using room background lines and a standard ${}^{152}\text{Eu}$ γ -ray source ($E_\gamma = 0.5$ –2.6 MeV). The data were acquired in an event-by-event mode, and subsequently the total

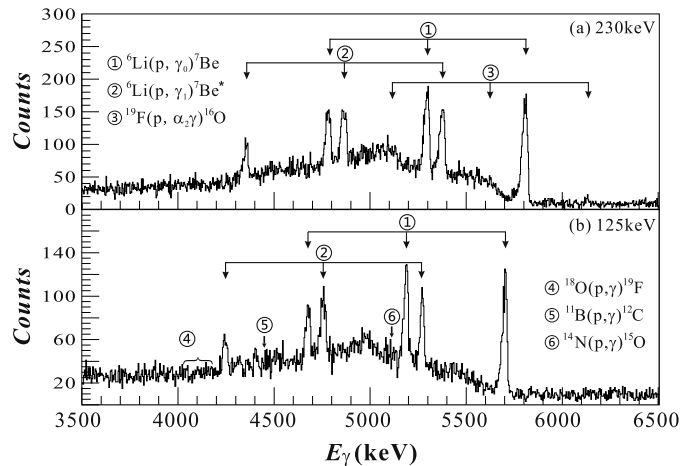


Fig. 1. Sample γ -ray spectra from the $p + {}^6\text{Li}$ radiative capture reaction obtained at energies of (a) $E_p = 230$ keV, and (b) $E_p = 125$ keV. See text for details.

γ -ray energy spectrum at each energy was obtained by summing those calibrated spectra detected in four segments. An EJ-200 plastic scintillator [28] (length = 100 cm, width = 50 cm, thickness = 5 cm) was placed 10 cm above the Clover detector and the coincidence signals between both detectors were rejected. This reduced the cosmic-ray background by roughly factors of 2–3 in the relevant energy range of the primary capture γ rays of ${}^6\text{Li}(p, \gamma){}^7\text{Be}$ [26]. An ORTEC ULTRA Ion-Implanted Silicon Detector [29] with a 4 mm in diameter collimator was installed at 135° with respect to the beam direction at a distance of 10 cm from the target, which was used for detecting the ${}^3\text{He}$ and α particles from the ${}^6\text{Li}(p, \alpha){}^3\text{He}$ reaction. In order to stop the intense elastically scattered protons, a gold foil of 1.7 μm thickness was placed in front of the detector. The Si detector was insulated electrically from the target chamber.

The sample γ -ray spectra from the $p + {}^6\text{Li}$ radiative capture reaction obtained at energies of $E_p = 125, 230$ keV are shown in Fig. 1. The γ transitions to the ground state (γ_0) and to the first excited state (γ_1) in ${}^7\text{Be}$ are clearly observed. Fig. 1(b) also indicates the expected positions of the possible contaminant γ rays from the (p, γ) reactions on ${}^{11}\text{B}$, ${}^{14}\text{N}$ and ${}^{18}\text{O}$, and no visible background γ rays were found. Due to a small contamination in the Ta backing, the 6.13 MeV γ rays from the ${}^{19}\text{F}(p, \alpha\gamma){}^{16}\text{O}$ reaction appeared in our region of interest above ~ 184 keV. In an additional measurement run with a LiF target, the fluorine contribution arising from the Compton background and escaped peaks of the 6.13 MeV γ rays was normalized to the photo-peak of 6.13 MeV γ rays. With this normalization factor, the fluorine contribution in our region of interest was thus subtracted accordingly. The summing effect of the cascade transitions for the segmented Clover detectors is estimated to be about 1%. We have utilized two methods for extracting the γ capture yields: yields only from the photo-peak of γ_0 , and yields from the integrated region of the spectra from the double-escape peak of the γ_1 -transition up to the photo-peak of the γ_0 transition. Fig. 2 shows the relative ratio of photo-peak γ -ray yields of the ground-state (γ_0) and first-excited-state (γ_1) captures. The ratio is about 1.57 ± 0.15 averaging over the measured energy region shown in Fig. 2, which is well consistent with the previous value of 1.56 ± 0.10 [8]. In fact, this branching ratio was previously determined to be nearly a constant in the energy region of $E_p = 0.4$ –1.0 MeV [30–33]. Note, in Figs. 2–6 the energies shown are the effective $E_{\text{c.m.}}$ energies corrected for the target thickness effect [1]. Since the integration method gives better statistics at low-energy points than the γ_0 method, some extra

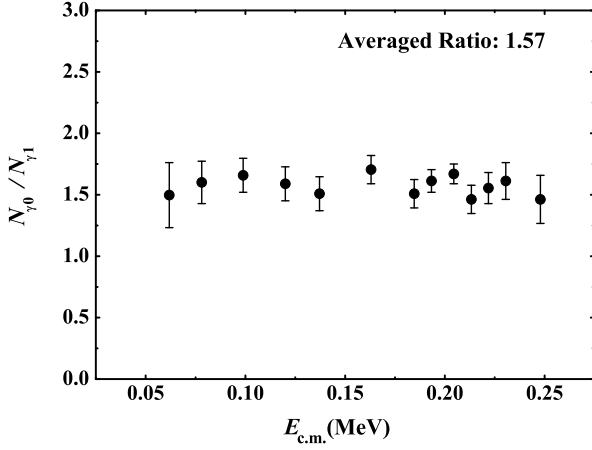


Fig. 2. Yield ratios between the ground-state (γ_0) and the first-excited-state (γ_1) captures for the ${}^6\text{Li}(p, \gamma){}^7\text{Be}$ reaction. The errors shown are only the statistical ones. Note, the $E_{c.m.}$ energies shown in the following Figs. 3–6 are also corrected by the target thickness effect [1].

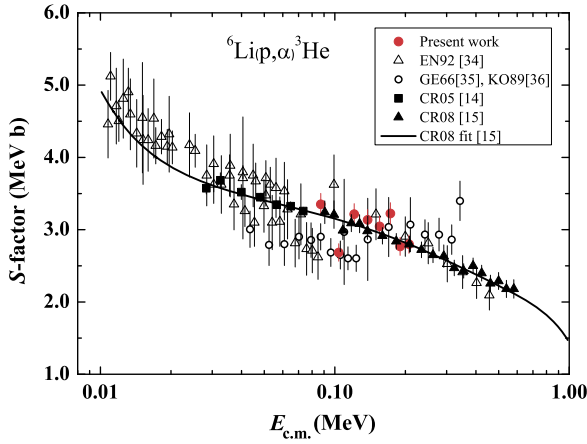


Fig. 3. (Color online.) Astrophysical S -factor data of ${}^6\text{Li}(p, \alpha){}^3\text{He}$ as function of energy. The (red) solid data points are from present work. The previous data are also shown for comparison, where the filled triangle data points are from Ref. [15], the rectangular ones from Ref. [14], the hollow triangle ones from Ref. [34], and the hollow circle ones from Ref. [35,36], respectively.

data at lower energies are obtained. It is found that both data fitted with each other very well, and it illustrates the integration method utilized is reliable in our energy region of interest (see following paragraph). Such consistency of comparison again supports the constant γ_0/γ_1 branching ratio in the energy region studied. In addition, in this measurement, no serious target deterioration was observed by monitoring the γ -ray yields at the $E_{c.m.} = 206$ keV energy point in several runs over the entire experiment, for a totally accumulated charge of 6 C. The ratio between the γ_0 yield and the accumulated charge is quite stable, fluctuating only about $\pm 2\%$.

The present S factors of ${}^6\text{Li}(p, \alpha){}^3\text{He}$ have been normalized to the recent precise data of Cruz et al. [15] at one energy point of $E_{c.m.} = 206$ keV. The S factors are shown in Fig. 3, where the (red) solid data points represent the present results. The uncertainty mainly arises from that of the Cruz et al.'s S factor, while the statistical one is negligible. It shows that our data are well consistent with the previous data within the uncertainties, except for one data point at $E_{c.m.} = 104$ keV. In addition, the γ -ray-to- α -particle branching ratio $\text{BR}(E)$ has been determined via the equation [1, 10]

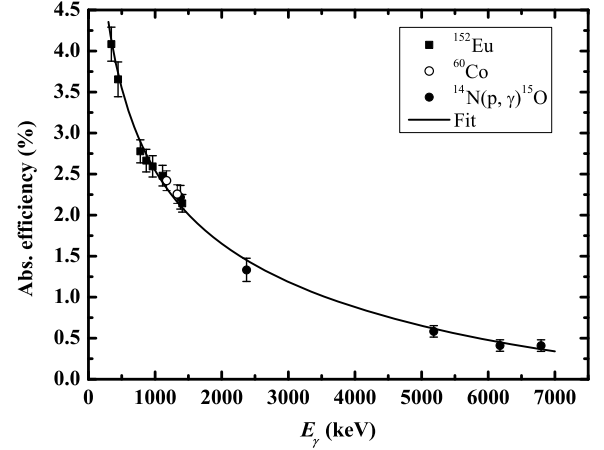


Fig. 4. The absolute efficiency calibrated for the Clover detector. The theoretical fitting curve [37] is also shown.

$$\text{BR}(E) = \frac{N_{\gamma}}{N_{\alpha}} \approx \frac{\epsilon_{\alpha}}{\epsilon_{\gamma}} \times \frac{S_{(p, \gamma)}(E)}{S_{(p, \alpha)}(E)}. \quad (1)$$

Here, N_{α} , N_{γ} denote the total counts of α particle and γ rays from the respective ${}^6\text{Li}(p, \alpha){}^3\text{He}$ and ${}^6\text{Li}(p, \gamma){}^7\text{Be}$ channels detected in each energy run. The values ϵ_{α} , ϵ_{γ} represent the absolute detection efficiency of the Si and Clover detectors, respectively. The efficiency ϵ_{α} depends only on the solid angle covered by the Si detector. Similar to the work of Cecil et al., a decreasing branching ratio $\text{BR}(E)$ towards lower energies is also observed in this work.

In this work, the absolute efficiency of the Clover was calibrated by two standard ${}^{152}\text{Eu}$ and ${}^{60}\text{Co}$ sources with known activities, as well as by the γ rays from a ${}^{14}\text{N}(p, \gamma){}^{15}\text{O}$ experiment in which a 2 mm N_4Si_3 thick target was bombarded by a 280 keV proton beam. The relative efficiencies for the γ rays at 2373, 5183, 6176, and 6793 keV were normalized to the 1380 keV line, and all these relative efficiencies subsequently normalized to the absolute efficiency curve determined by the standard ${}^{152}\text{Eu}$ and ${}^{60}\text{Co}$ sources. The experimental efficiency data points and a theoretical fitting curve [37] are shown in Fig. 4. The details of the efficiency calibration including a GEANT4 simulation [38] will be published elsewhere [26]. A ratio of $\frac{N_{\gamma}/\epsilon_{\gamma}}{N_{\alpha}/\epsilon_{\alpha}}$ is determined to be $(3.14 \pm 0.28) \times 10^{-5}$ at the energy of $E_{c.m.} = 206$ keV. Here, the error mainly originates from those of the γ_0/γ_1 branching ratio (6.4% [8]) and the γ detection efficiency ($\sim 5\%$). At 206 keV, the ${}^6\text{Li}(p, \alpha){}^3\text{He}$ angular distribution was known to be anisotropic [34, 36,39], and a ratio $A_1/A_0 = 0.21 \pm 0.01$ was deduced based on the compiled data in Ref. [34] with a second-order polynomial fit. With the precise S factor of Cruz et al. [15], an S factor of the ${}^6\text{Li}(p, \gamma){}^7\text{Be}$ reaction is determined to be $S = 93.4 \pm 10.5$ eV \cdot b at this energy point with Eq. (1), by taking the ${}^6\text{Li}(p, \alpha){}^3\text{He}$ angular distribution into account. The quoted error arises mainly from the uncertainties in the statistics ($\sim 1.5\%$), the Cruz et al.'s S factor ($\sim 4\%$), the (p, α) angular distribution effect ($\sim 5\%$), and the $\frac{N_{\gamma}/\epsilon_{\gamma}}{N_{\alpha}/\epsilon_{\alpha}}$ ratio ($\sim 9\%$). All other S factors are subsequently normalized to this S factor. The derived S factors of the ${}^6\text{Li}(p, \gamma){}^7\text{Be}$ reaction are shown in Fig. 5, where the solid circles represent the S factors determined by the yields only from the photo-peak of γ_0 , and the hollow circles represent the ones by the yields from the integration method. It indicates that two values are consistent within the uncertainties. It shows that the ${}^6\text{Li}(p, \gamma){}^7\text{Be}$ S factor declines with decreasing energy at low energies. Here, the capture γ rays are assumed to be isotropic [33,40] in our narrow energy range. This assumption is based on the transition selection rule [41] discussed

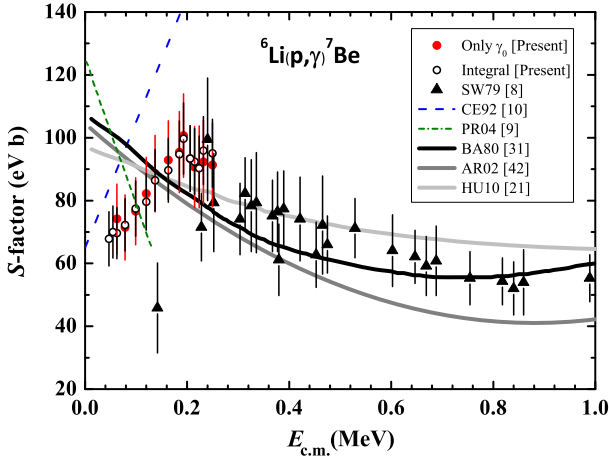


Fig. 5. (Color online.) Astrophysical S factors of ${}^6\text{Li}(p, \gamma){}^7\text{Be}$ as function of energy. The solid circles represent the S factors determined by the yields only from the photo-peak of γ_0 , and the hollow circles represent the ones by the yields from the integration method. The triangular data points are from previous work and the solid points from present work. The solid lines represent previous theoretical calculation results [31,42,21]. The total S -factor curves of Cecil et al. [10] and Prior et al. [9] are also shown for comparison.

below. The dominant $E1$ transition requires the s - ($s \rightarrow p$) or d -wave ($d \rightarrow p$) proton captures on ${}^6\text{Li}$, where the contribution from the above d -wave capture can usually be neglected [41] at energies well below the Coulomb barrier (~ 1.1 MeV). Therefore, such an s -wave dominated $E1$ transition in ${}^6\text{Li}(p, \gamma){}^7\text{Be}$ should show an isotropic angular distribution in the energy region studied. This isotropic assumption was also utilized in the work of Cecil et al.

Our data are consistent with Switkowski et al.'s ones obtained around $E_{\text{c.m.}} \sim 200$ keV, but inconsistent, at the lower energies, with calculations of the direct capture models [21,31] and of the cluster microscopic models [42,43]. In addition, Switkowski et al.'s lowest data point at 140 keV is about 1.8 times smaller than the present value. The total S -factor curves of Cecil et al. and Prior et al. are also shown for comparison. Although the trend of Cecil et al.'s S factors is similar to ours, their values considerably deviate from ours and Switkowski et al.'s. This deviation is probably caused by their isotropic assumption of the (p, α) angular distribution. In fact, their data will be consistent with ours by taking the actual angular distribution.

A resonance-like structure appears in our ${}^6\text{Li}(p, \gamma){}^7\text{Be}$ S -factor data as shown in Fig. 5. As the capture process at higher energies is dominated by the direct capture amplitude $E1(s \rightarrow p)$, the possible interference effect requires a resonance with $J^\pi = 1/2^+$ or $3/2^+$. The existence of positive parity states in the range of this work has been a question long time ago. For example, many low-lying, positive-parity states in ${}^7\text{Be}$ were predicted previously [11] by using configurations of $(1s)^4(1p)^22s$, $(1s)^4(1p)^21d$. However, earlier experiments on ${}^7\text{Be}$ and its mirror ${}^7\text{Li}$ have found no clear evidence for a positive parity level within the energy range investigated. The R -matrix [44] calculations have been done with an AZURE code [45] by assuming a positive-parity resonance [$E_R \approx 195$ keV, $J^\pi = (1/2^+, 3/2^+)$, $\Gamma_p \approx 50$ keV], and the theoretical results can roughly explain the observed structure as shown in Fig. 6. Additionally the preliminary results from a recent potential model calculation [46] coupling with an s -wave resonance can also explain the observed S factors. With regard to the angular distribution of ${}^6\text{Li}(p, \alpha){}^3\text{He}$, Engstler et al. [34] gave a dominant coefficient A_1 and a negligible small A_2 . As discussed in Refs. [15, 47], the R -matrix fit on these data would require contributions from both positive- and negative-parity levels of ${}^7\text{Be}$, presumably

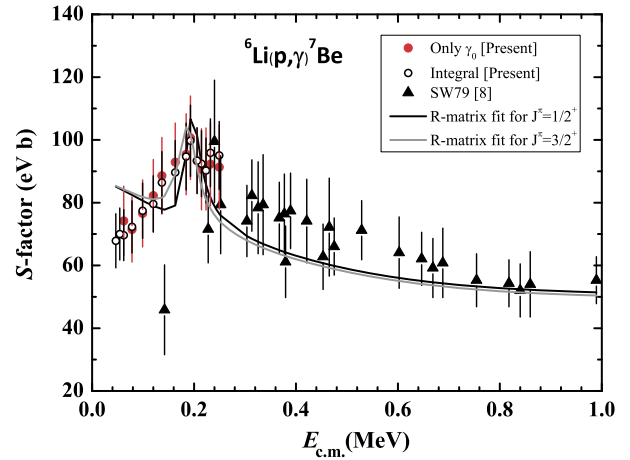


Fig. 6. (Color online.) R -matrix fits for the astrophysical S factors of ${}^6\text{Li}(p, \gamma){}^7\text{Be}$. A low-energy resonance is assumed in the calculation. The resonance parameters are $E_R \approx 195$ keV, $J^\pi = (1/2^+, 3/2^+)$ and $\Gamma_p \approx 50$ keV.

formed by s - and p -wave protons. However, one cannot obtain any contribution to A_1 from $5/2^-$ and $1/2^+$ levels; a nonzero A_1 requires $3/2^+$, $5/2^+$ or $7/2^+$ levels together with the $5/2^-$ levels (for 6.73 and 7.21 MeV states). This might indicate that the possible new resonance is a $3/2^+$ state. Actually, such $3/2^+$ excited states were observed around $E_x = 3.4$ – 4.7 MeV in the neighbor ${}^9\text{Be}$, ${}^{11}\text{Be}$ and ${}^9\text{B}$ nuclei [48]. However, the existence of such a resonance (either in ${}^7\text{Be}$ in or ${}^7\text{Li}$) is still uncertain and requires to be clarified in the future detailed investigations. For example, a resonant elastic-scattering experiment of ${}^6\text{Li} + p$ is being considered for searching such an interesting resonance. A tentative appearance of a ‘dip’-like resonance structure around 200 keV were observed in the earlier ${}^6\text{Li}(p, \alpha){}^3\text{He}$ experiments [35,36] (as shown in Fig. 3). A recent paper [49], which was published during the refereeing process for this Letter, reported updated S factors for the reaction by using the Trojan Horse method [50]; no such ‘dip’-like resonance structure was observed. One lower S -factor data point presently observed at $E_{\text{c.m.}} = 104$ keV is not sufficient to clarify this issue, and therefore a careful study of this ${}^6\text{Li}(p, \alpha){}^3\text{He}$ reaction is now under consideration with our setup.

In addition, the major component of the ground state of ${}^6\text{Li}(1^+)$ is ${}^4\text{He}(0^+)$ plus $D(S=1, L=0)$ in a relative s -wave between ${}^4\text{He}$ and D . However, it is well known that 4–7% in probability [51–53] of the ground state of deuteron consists of d -wave, i.e., $D(S=1, L=2)$ for the tensor interaction. This component can make the ground state of ${}^6\text{Li}(1^+)$ as ${}^4\text{He}(0^+)$ plus $D(S=1, L=2)$ in a relative d -wave, and possibly cause a decreasing behavior of the S factor as the energy decreases [54]. Since the low-energy ${}^6\text{Li}(p, \alpha){}^3\text{He}$ S factor does not exhibit such a sizable decline but is characterized by an S factor slowly increasing with decreasing energy [34] – as was also confirmed in the present work – the sizable drop in the capture reaction is most likely not an effect of the entrance channel. The complicated coupled-channel model calculation is however beyond the scope of this Letter.

In the astrophysical aspects, the observed decline in ${}^6\text{Li}(p, \gamma){}^7\text{Be}$ cross sections at energies below 200 keV also leads to a reduction of the reverse rate ${}^7\text{Be}(\gamma, p){}^6\text{Li}$ through the detailed balance theory. We calculated the effect of the difference in low-energy cross section of ${}^6\text{Li}(p, \gamma){}^7\text{Be}$ on the SUSY assisted BBN model by adopting the same parameters as in Ref. [20], where a long-lived radiatively decaying particle was assumed to exist in the early Universe. Light element abundances could be affected through non-thermal nucleosynthesis triggered by photons which were produced in the decay with energy much larger than

photo-disintegration thresholds of all light nuclei as assumed in all studies excepting Ref. [55]. We have verified that the final yields of ${}^7\text{Be}$ and ${}^6\text{Li}$ do not change significantly as expected with our new data; effects on the ${}^6\text{Li}$ abundance depend on the energy of photons emitted at the decay [55] since there are several reaction paths for the ${}^6\text{Li}$ production with different threshold energies.

As for the anomalous behavior in low-energy cross section of the ${}^6\text{Li}(p, \gamma){}^7\text{Be}$ reaction, the exact nature of the possible novel reaction mechanism or a new low-energy resonance leading to such a declining effect remains unknown and requires more detailed experimental and theoretical characterization. This case shows again the danger of simply extrapolating experimental data over a very large energy range towards stellar energies. It also demonstrates the necessity for carefully studying the low-energy reaction cross sections, which might be helpful for discovering new physics and important astrophysical implications.

Acknowledgements

We wish to thank engineers for operating the 320 kV platform. J.J. would like to express appreciation to Shigeru Kubono and Daïd Kahl (CNS, University of Tokyo) who made helpful comments on the manuscript. This work was financially supported by the National Natural Science Foundation of China (Nos. 11135005, 11021504), the Major State Basic Research Development Program of China (2013CB834406) and the “100 Persons Project” (BR091104) of Chinese Academy of Sciences. C.R. was supported by the Visiting Professorships Program of CAS and the Joint Institute for Nuclear Astrophysics at the University of Notre Dame (NSF-Phys-0822648). T.K. was supported in part by the Grants-in-Aid for Scientific Research of the JSPS (20244035) and Scientific Research on Innovative Area of MEXT (2010544).

References

- [1] C.E. Rolfs, W.S. Rodney, *Cauldrons in the Cosmos*, University of Chicago Press, 1988.
- [2] C. Angulo, et al., *Nucl. Phys. A* 565 (1999) 3.
- [3] C. Broggini, et al., *Annu. Rev. Nucl. Part. Sci.* 60 (2010) 53.
- [4] W.A. Fowler, *Rev. Mod. Phys.* 56 (1984) 149.
- [5] W.D. Arnett, J.W. Truran, *Nucleosynthesis – Challenges and New Developments*, University of Chicago Press, 1985.
- [6] F.J. Wilkinson, F.E. Cecil, *Phys. Rev. C* 31 (1985) 2036.
- [7] C.A. Barnes, et al., *Phys. Lett. B* 197 (1987) 315.
- [8] Z.E. Switkowski, et al., *Nucl. Phys. A* 331 (1979) 50.
- [9] R.M. Prior, et al., *Phys. Rev. C* 70 (2004) 055801.
- [10] F.E. Cecil, et al., *Nucl. Phys. A* 539 (1992) 75.
- [11] A.M. Lane, *Rev. Mod. Phys.* 32 (1960) 519.
- [12] S. Bashkin, R.R. Carlson, *Phys. Rev.* 97 (1955) 1245.
- [13] J.B. Marion, et al., *Phys. Rev.* 104 (1956) 1402.
- [14] J. Cruz, et al., *Phys. Lett. B* 624 (2005) 181.
- [15] J. Cruz, et al., *J. Phys. G: Nucl. Part. Phys.* 35 (2008) 014004.
- [16] D.D. Clayton, *Principles of Stellar Evolution and Nucleosynthesis*, University of Chicago Press, 1983.
- [17] P.J.E. Peebles, et al., *Nature (London)* 352 (1991) 769.
- [18] C.J. Copi, et al., *Science* 267 (1995) 192.
- [19] D.N. Schramm, R. Wagoner, *Annu. Rev. Nucl. Part. Sci.* 27 (1977) 37.
- [20] M. Kusakabe, et al., *Phys. Rev. D* 74 (2006) 023526.
- [21] J.T. Huang, et al., *At. Data Nucl. Data Tables* 96 (2010) 824.
- [22] G. Audi, et al., *Nucl. Phys. A* 729 (2003) 337.
- [23] L.T. Sun, et al., *Nucl. Instr. Meth. B* 263 (2007) 503.
- [24] X. Ma, et al., *J. Phys.: Conf. Ser.* 163 (2009) 012104.
- [25] M. Wiescher, et al., *Nucl. Phys. A* 349 (1980) 165.
- [26] S.Z. Chen, et al., *Nucl. Instr. Meth. A* (2013), in preparation.
- [27] CANBERRA Germanium detectors, <http://www.canberra.com/>.
- [28] ELJEN Technology, <http://www.eljentechnology.com/>.
- [29] Advance Measurement Technology (AMETEK), <http://www.ortec-online.com/>.
- [30] J.B. Warren, et al., *Phys. Rev.* 101 (1956) 242.
- [31] F.C. Barker, *Aust. J. Phys.* 33 (1980) 159.
- [32] R. Ostojčić, et al., *Nuovo Cimento* 70A (1983) 73.
- [33] C.I.W. Tingwell, et al., *Aust. J. Phys.* 40 (1987) 319.
- [34] S. Engstler, et al., *Z. Phys. A* 342 (1992) 471.
- [35] W. Gemeinhardt, et al., *Z. Phys.* 197 (1966) 58.
- [36] J.U. Kwon, et al., *Nucl. Phys. A* 493 (1989) 112.
- [37] D.C. Radford, *Nucl. Instr. Meth. A* 361 (1995) 297.
- [38] GEANT4, A toolkit for the simulation of the passage of particles through matter developed at CERN, <http://geant4.cern.ch/>.
- [39] A.J. Elwyn, et al., *Phys. Rev. C* 20 (1979) 1984.
- [40] F. Ajzenberg-Selove, *Nucl. Phys. A* 490 (1988) 1.
- [41] C.E. Rolfs, *Nucl. Phys. A* 217 (1973) 29.
- [42] K. Arai, et al., *Nucl. Phys. A* 699 (2002) 963.
- [43] S.B. Dubovichenko, et al., *Phys. At. Nucl.* 74 (2011) 984.
- [44] A.M. Lane, R.G. Thomas, *Rev. Mod. Phys.* 30 (1958) 257.
- [45] R.E. Azuma, et al., *Phys. Rev. C* 81 (2010) 045805.
- [46] K. Takahashi, Y. Xu, for NACRE II compilation (private communications).
- [47] F.C. Barker, *Nucl. Phys. A* 707 (2002) 277.
- [48] TUNL Nuclear Data Evaluation, <http://www.tunl.duke.edu/nucldata/>.
- [49] L. Lamia, et al., *Astrophys. J.* 768 (2013) 65.
- [50] G. Baur, *Phys. Lett. B* 178 (1986) 135.
- [51] J.N. Bahcall, R.M. May, *Astrophys. J.* 155 (1969) 501B.
- [52] R.B. Wiringa, et al., *Phys. Rev. C* 51 (1995) 38.
- [53] R. Machleidt, *Phys. Rev. C* 63 (2001) 024001.
- [54] T. Kajino, et al., *Suppl. J. Phys. Soc. Japan* 58 (1989) 639.
- [55] M. Kusakabe, et al., *Phys. Rev. D* 87 (2013) 085045.